



# Investigating the synergistic potential of Si and biochar to immobilize Ni in a Ni-contaminated calcareous soil after *Zea mays* L. cultivation

Hamid Reza Boostani<sup>1</sup>, Ailsa G. Hardie<sup>2</sup>, Mahdi Najafi-Ghiri<sup>1</sup>, Ehsan Bijanzadeh<sup>3</sup>, Dariush Khalili<sup>4</sup>, and Esmaeil Farrokhnejad<sup>1</sup>

<sup>1</sup>Department of Soil Science, College of Agriculture and Natural Resources of Darab, Shiraz University, Darab 74591, Iran

<sup>2</sup>Department of Soil Science, Faculty of AgriSciences, Stellenbosch University, Private Bag X1, Matieland 7602, South Africa

<sup>3</sup>Department of Agroecology, College of Agriculture and Natural Resources of Darab, Shiraz University, Darab 74591, Iran

<sup>4</sup>Department of Chemistry, College of Sciences, Shiraz University, Shiraz 71454, Iran

**Correspondence:** Hamid Reza Boostani (hr.boostani@shirazu.ac.ir)

Received: 13 November 2023 – Discussion started: 12 January 2024

Revised: 12 May 2024 – Accepted: 21 May 2024 – Published: 9 July 2024

**Abstract.** In Iran, a significant percentage of agricultural soils are contaminated with a range of potentially toxic elements (PTEs), including Ni, which need to be remediated to prevent their entry into the food chain. Silicon (Si) is a beneficial plant element that has been shown to mitigate the effects of PTEs on crops. Biochar is a soil amendment that sequesters soil carbon and that can immobilize PTEs and enhance crop growth in soils. No previous studies have examined the potentially synergistic effect of Si and biochar on the Ni concentration in soil chemical fractions and the immobilization thereof. Therefore, the aim of this study was to examine the interactive effects of Si and biochar with respect to reducing Ni bioavailability and its corresponding uptake in corn (*Zea Mays*) in a calcareous soil. A 90 d factorial greenhouse study with corn was conducted. Si application levels were 0 (S<sub>0</sub>), 250 (S<sub>1</sub>), and 500 (S<sub>2</sub>) mg Si kg<sup>-1</sup> soil, and biochar treatments (3wt %) including rice husk (RH) and sheep manure (SM) biochars produced at 300 and 500 °C (SM300, SM500, RH300, and RH500) were utilized. At harvest, the Ni concentration in corn shoots, the Ni content in soil chemical fractions, and the release kinetics of DPTA (diethylenetriaminepentaacetic acid)-extractable Ni were determined. Simultaneous utilization of Si and SM biochars led to a synergistic reduction (15 %–36 %) in the Ni content in the soluble and exchangeable fractions compared with the application of Si (5 %–9 %) and SM (5 %–7 %) biochars separately. The application of Si and biochars also decreased the DPTA-extractable Ni and Ni content in corn shoots (by up to 57 %), with the combined application of SM500 + S<sub>2</sub> being the most effective. These effects were attributed to the transfer of Ni in soil from more bioavailable fractions to more stable iron-oxide-bound fractions, related to soil pH increase. SM500 was likely the most effective biochar due to its higher alkalinity and lower acidic functional group content which enhanced Ni sorption reactions with Si. The study demonstrates the synergistic potential of Si and SM biochar for immobilizing Ni in contaminated calcareous soils.

## 1 Introduction

One of the most important ways for potentially toxic elements (PTEs) to enter the human food chain is through the consumption of plants grown in soils contaminated with PTEs. Potentially toxic elements pollute soil environments as a result of mining, metal smelting, and the use of sewage sludge and domestic and industrial effluents in agriculture, especially in developing countries (Liu et al., 2018). Potentially toxic elements in soils cannot undergo biodegradation by living organisms, so they possess great stability and longevity in the soil (Poznanović Spahić et al., 2019). Unlike other PTEs found in soils, such as mercury (Hg), cadmium (Cd), and lead (Pb), nickel (Ni) is essential for plant growth at very low concentrations. Nevertheless, at elevated contents ( $> 35 \text{ mg Ni kg}^{-1}$  soil), Ni causes many physiological and morphological malfunctions in plants and severely stunts their growth (Shahzad et al., 2018; Antoniadis et al., 2017). In a study conducted by Shahbazi et al. (2022), the Ni-weighted average concentration of the cultivated lands of Iran in the vicinity of industrial areas was reported to be  $350 \text{ mg kg}^{-1}$  soil. In these soils, the pollution index (the ratio of the element concentration to the standard concentration) calculated for Ni is greater than 5, which indicates a severe degree of pollution from the point of view of environmental protection. Shahbazi et al. (2020) collected 711 agricultural soil samples from locations in different climate zones (extra arid, arid, semi-arid, Mediterranean, semi-humid, humid, and per-humid based on the de Martonne classification system) of Iran and reported that the Ni content in the soils was between  $2.79$  and  $770 \text{ mg kg}^{-1}$  with an average of  $68 \text{ mg kg}^{-1}$  soil. The results showed that the concentration of Ni in 11.3% of these soils was higher than the threshold value. Removing PTEs from contaminated sites via traditional methods, such as pump and treat technologies, soil washing, and excavation, is very expensive and time-consuming; therefore, for plant cultivation in these areas, low-cost and effective methods should be sought to stabilize PTEs in soils and prevent them from being transferred to plants (Gao et al., 2023).

Silicon (Si) is a valuable nutrient for plant growth, although it is only considered essential for some plant species, such as rice. Applying Si to the soil can enhance plant resistance against biological and non-biological stressors, including physiological stress caused by PTEs in soil (Bhat et al., 2019; Yan et al., 2018). The use of Si to promote plant growth and mitigate the toxicity of PTEs is becoming increasingly popular in agriculture (Li, 2019; Adrees et al., 2015). The application of Si in soils contaminated with PTEs may reduce the bioavailability of PTEs by increasing soil pH; increasing the secretion of organic ligands by the roots and the formation of insoluble compounds with PTEs; and, ultimately, enhancing plant growth (Bhat et al., 2019; Xiao et al., 2021). The soil pH increase associated with Si application is attributed to the hydrolysis reaction of the silicate anion in soil solution, which generates hydroxyl ions (Ma et al., 2021).

Biochar can be used for a number of applications, including as a soil amendment that sequesters soil carbon (C) and for the stabilization of PTEs in polluted sites (El-Naggar et al., 2018). Biochar is a carbon-rich, porous organic material that is prepared under limited- or no-oxygen conditions via the pyrolysis of organic wastes, including crop and animal residues, urban waste, and wood byproducts (Vickers, 2017; Ankita Rao et al., 2023). The organic surface functional groups of biochar, such as carboxylic and phenolic groups, provide cation exchange capacity in soils (Tomczyk et al., 2020). The addition of biochar to the soil not only improves the soil chemical and physical properties but also reduces the bioavailability of PTEs in contaminated soils through some physicochemical processes such as sedimentation, complexation, and electrostatic adsorption (Bandara et al., 2020; Deng et al., 2019; Derakhshan Nejad et al., 2018). The complexation of Ni with oxygen-containing functional groups on biochar surfaces including carboxyl, ether, carbonyl, and hydroxyl has been identified as a key mechanism for Ni immobilization in soil (Alam et al., 2018; El-Naggar et al., 2018). Electrostatic attraction of Ni by negatively charged functional groups on the surfaces of biochar is another potential mechanism for Ni stabilization in soil (Ahmad et al., 2014). Increased soil pH following the application of biochar also promotes Ni adsorption reactions (Uchimiya et al., 2010). However, the efficiency of biochar prepared from different feedstocks and under different production conditions with respect to stabilizing PTEs in soils can vary significantly (Dey et al., 2023).

Potentially toxic elements in soil can exist in different chemical fractions, such as the water-soluble and exchangeable (WsEx) fraction, bound to carbonates (Car), bound to organic matter (OM), bound to iron and manganese oxides ( $\text{FeMnO}_x$ ), and the residual (Res) fraction (found in minerals) (Singh et al., 1988). The bioavailability of these forms differs: the WsEx fraction has the highest bioavailability, whereas the Res form is considered unusable by plants. PTEs in other chemical fractions in soils could be potentially accessible for plant roots depending on soil characteristics such as soil texture, soil pH, and soil organic matter content (Kamali et al., 2011; Bharti et al., 2018). Diethylenetriamine-pentaacetic acid (DTPA) extraction is commonly employed for assessing Ni availability in calcareous soils (Lindsay and Norvell, 1978). However, it is important to acknowledge that this methodology solely assesses Ni availability for plants, while the quantity of released Ni may vary across distinct stages of plant development. Consequently, the examination of alterations in extractable Ni levels over time using the DTPA solution can prove valuable in estimating the bioavailability of Ni in soil. The PTE desorption capacities of soils are anticipated to be contingent upon factors such as soil pH, cation exchange capacity, the specific nature of metal ions, and the source of the metals (Kandpal et al., 2005). Furthermore, the release kinetics parameters can provide insight into the bonding mechanisms of PTEs in soils and their

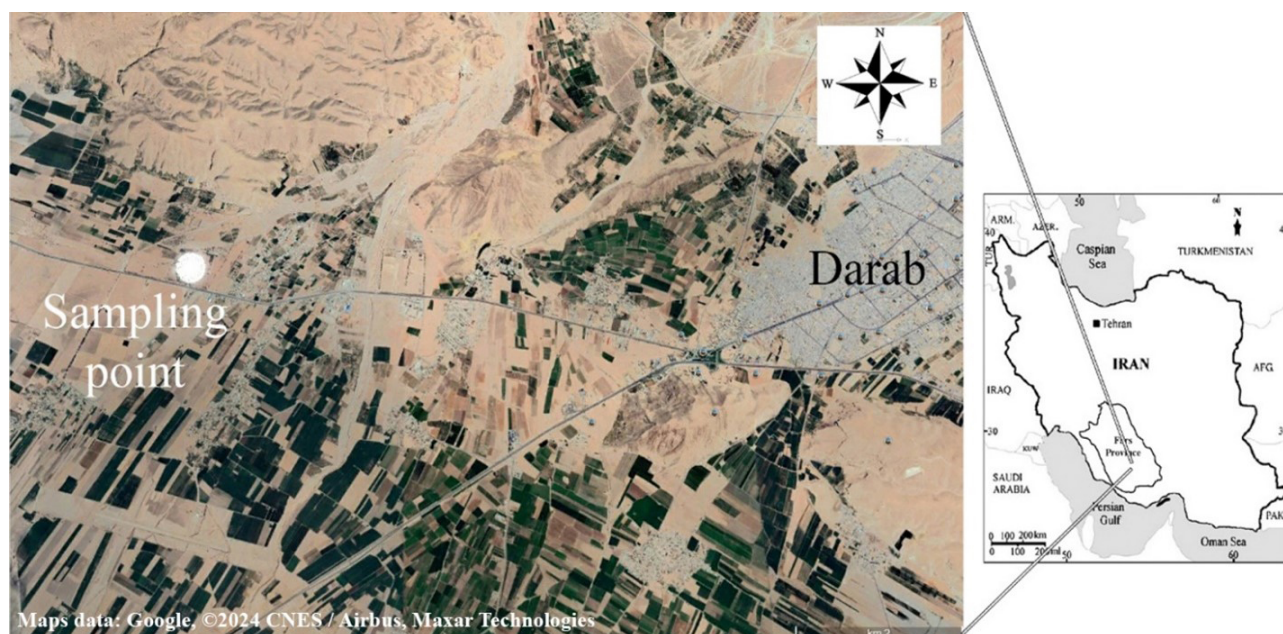


**Figure 1.** The soil sampling location in the Darab region, southern Iran.

potential risk for leaching into groundwater or surface water (El-Naggar et al., 2021). Therefore, sequential extraction methods and release kinetics models have been employed to assess the efficacy of amendment materials with respect to stabilizing PTEs in contaminated soils. Xiao et al. (2021) found that the addition of mineral Si fertilizer to a contaminated paddy soil caused a significant decrease in the Cd and Pb fractions bound to carbonates and iron–manganese oxides, while the residual and organic-matter-bound forms experienced a notable increase. In another study, the application of cotton residue biochar (1.5 wt %) to a calcareous soil with a sandy loam textural class containing different levels of Cd contamination was more efficacious than corn and wheat straw biochars with respect to decreasing the Cd content in the WsEx and Car fractions and enhancing the Cd concentration in the Res fraction. In addition, the application of cotton residue biochar decreased the EDTA (ethylenediaminetetraacetic acid)-extractable Cd by 45 %–52 % compared with the control (Boostani et al., 2023b).

As both biochars and Si are economical and effective soil amendments to reduce plant uptake of PTEs and stress in contaminated soils, their potential synergistic effect on the immobilization of PTEs in soils should be further investigated. Currently, no previous studies have examined the combined application effects of Si and biochars on the Ni content in various soil chemical fractions or the release kinetics of Ni in calcareous soils. Thus, the primary objective of the present study was to elucidate the interaction of biochars and Si levels with respect to reducing the bioavailability of Ni in soil and its corresponding accumulation in corn (*Zea Mays* L. 604). Additionally, the study sought to elucidate the underly-

ing soil chemical mechanisms that are likely to be responsible for such effects.

## 2 Materials and methods

### 2.1 Soil sampling, characterization, and Ni treatment

A composite soil sample from the surface layer (0–30 cm) was collected with an auger at the research farm of the College of Agriculture and Natural Resources in Darab, southern Iran (28°45′0.99″ N, 54°26′52.14″ E; 1105 m elevation; Fig. 1). The climate, mean annual precipitation, soil moisture regime, and thermal regime of the studied area were semi-arid, 250 mm, ustic, and hyperthermic, respectively. The composite soil sample was placed in polyethylene bags in the field and then transported to laboratory; upon arrival at the laboratory, it was immediately air-dried, passed through a 2 mm sieve, and stored at room temperature until the physicochemical analysis was performed. Soil sand, silt, and clay content values were determined by the hydrometer method (Gee and Bauder, 1986). Soil pH and electrical conductivity (EC) were determined using a saturated paste (Rhoades, 1996), while organic matter was determined using the Walkley–Black procedure (Nelson and Sommers, 1996). The calcium carbonate equivalent (CCE) was determined by acid neutralization (Loeppert and Suarez, 1996), while the cation exchange capacity was determined using 1 M ammonium acetate (Merck, 99 %) method (Sumner and Miller, 1996). Available Ni was determined using DPTA (diethylenetriaminepentaacetic acid; Merck, 99 %) extraction (Lindsay and Norvell, 1978). Plastic containers were filled with 2 kg

of soil, and 500 mL of  $\text{NiCl}_2$  (Merck, 99 %) solution was then mixed into the containers to achieve a Ni concentration of  $300 \text{ mg Ni kg}^{-1}$  soil. The Ni-treated soil samples were allowed to dry out at room temperature, rewetted to field capacity using deionized water, and then allowed to dry out again. The rewetting and room temperature drying cycle was repeated three times to allow the Ni to equilibrate with the soil. The repeated wetting and drying cycles were performed to simulate field processes (Boostani et al., 2023c). The incubation period was 60 d and the ambient temperature was  $25 \pm 2^\circ\text{C}$ .

## 2.2 Production of biochar and its properties

The respective sheep manure and rice husk samples were procured from active animal husbandry and a rice mill factory situated in the Darab region, Fars Province, Iran. Subsequently, the raw materials underwent a 1-week period of air-drying, followed by electrical milling and sieving through a 2 mm mesh. A slow pyrolysis procedure (2 h at 300 and  $500^\circ\text{C}$ , respectively) in an oxygen-limited environment was carried out to generate biochars from feedstocks (Anand et al., 2023). The generated biochars were then cooled at ambient temperature and sieved with a 0.5 mm mesh to ensure a consistent particle size. The chemical characteristics of the biochars were assessed using the following standard methods. Biochar pH and EC were determined in a 1 : 10 deionized water suspension (Sun et al., 2014), while cation exchange capacity (CEC) was determined using the method of Abdelhafez et al. (2014). Biochar total C, N, and H contents were determined by elemental analyser (ThermoFinnigan Flash EA 1112 Series, Thermo Fisher Scientific, USA). Biochar moisture and ash content were determined by heating in an oven, while the O + S content was calculated by subtraction of C, N, H, ash content, and moisture content from total biochar mass (Keiluweit et al., 2010). The biochar total Ni content was determined by combustion and dissolution of the ash in 2 M HCl (Merck, 37 %) (Boostani et al., 2018). The Ni content in the acid solution was determined using atomic absorption spectroscopy (AAS) (PG990, PG Instruments Ltd., UK). Surface functional groups of the biochars were assessed with Fourier transform infrared (FTIR) spectroscopy using a Shimadzu DR-8001 instrument and the KBr pellet transmission method. The morphology of surface biochar was assessed using scanning electron microscopy (SEM) (TESCAN VEGA3, Czech Republic).

## 2.3 Greenhouse experiment

A completely randomized factorial experiment was conducted in a greenhouse environment with three replications. The first factor consisted of the biochar treatments including rice husk (RH) and sheep manure (SM) generated at both 300 and  $500^\circ\text{C}$  (Control, C, with no biochar; SM300; SM500; RH300; and RH500), each at the level of 3wt % The sec-

ond factor included Si application levels ( $0 \text{ mg Si kg}^{-1}$  soil,  $S_0$ ;  $250 \text{ mg Si kg}^{-1}$  soil,  $S_1$ ; and  $500 \text{ mg Si kg}^{-1}$  soil,  $S_2$ ) supplied as  $\text{Na}_2\text{SiO}_3$  (98 %; Sigma Aldrich) solution. Based on the experimental design, Si levels were added to the 2 kg of Ni-treated soil samples. After drying the soil and mixing it, the prepared biochars were added to the required amount. Immediately after that, the treated soil samples were transferred to plastic pots (45 pieces, each containing 2 kg soil). To facilitate the required reactions, the moisture content of the samples was kept at the field capacity level for a duration of 2 weeks. Thereafter, six corn seeds (*Zea mays* L. 604) were planted in each pot; at the four-leaf stage, two plants were kept in each pot until the end of cultivation. During the growth of the plant, distilled water was used to maintain the soil moisture content in the pots at field capacity. After 90 d, the plants were harvested at the soil interface, rinsed with distilled water to remove contamination, immediately air-dried, and kept for Ni determination of plant shoots. After separating the roots, the soil from the pots was immediately air-dried, passed through a 2 mm sieve, and stored in labelled polyethylene bags at room temperature to be subsequently utilized for Ni sequential extraction and release kinetics analysis.

## 2.4 Sequential extraction procedure

The present study employed a successive extraction technique (Singh et al., 1988) to fractionate Ni into the water-soluble and exchangeable (WsEx), carbonate-bound (Car), organic-matter-bound (OM), manganese-oxide-bound ( $\text{MnO}_x$ ), amorphous-iron-oxide-bound ( $\text{AFeO}_x$ ), crystalline-iron-oxide-bound ( $\text{CFeO}_x$ ), and residual (Res) soil chemical fractions. The methodological specifics are provided in Table 1.

## 2.5 Release kinetics experiment

A 50 mL centrifuge tube was filled with 10 g of soil. After that, 20 mL of DTPA solution, 0.005 M DTPA (Merck, 99 %) + 0.1 M triethanolamine (Merck, 99 %) + 0.01 M calcium chloride (Merck, 97 %) (pH: 7.3) (Lindsay and Norvell, 1978), was added to the soil. The soil–DTPA mixtures were stirred for specific periods of time (i.e. 5, 15, 30, 60, 120, 360, 720, and 1440 min) at a constant temperature ( $25 \pm 2^\circ\text{C}$ ). After each stirring time, the soil suspension was centrifuged ( $2683 \times g$ ) to separate the soil particles from the liquid phase. Atomic absorption spectroscopy (AAS) (PG990, PG Instruments Ltd., UK) was used to analyse the Ni concentration in the liquid phase. The Ni concentration in the liquid phase versus time was plotted to obtain a Ni release kinetics curve. A total of seven kinetics models, namely, order models (zero, first, second, and third), parabolic diffusion models, power function models, and simple Elovich models, were assessed to fit the Ni release data. The best models for describing the data were selected according to the

**Table 1.** Successive extraction technique of Singh et al. (1988).

Chemical speciation containing Ni	Acronym	Duration of agitation (h)	Extractants	Relative density (g cm <sup>-3</sup> )
Exchangeable and soluble Carbonate	WsEx Car	2.0 5.0	1 M magnesium nitrate (Merck, 98 %) 1 M sodium acetate (Merck, 99 %, pH = 5)	1.10 1.04
Organic Mn oxide	OM MnO <sub>x</sub>	0.5 0.5	0.7 M sodium hypochlorite (pH = 8.5) 0.1 M hydroxyl amine hydrochloride (Merck, 98 %; Merck, 65 %, pH = 2 by nitric acid)	1.00 1.00
Amorphous Fe oxides	AFeO <sub>x</sub>	0.5	0.25 M hydroxyl amine hydrochloride (Merck, 98 %) + 0.25 M chloridric acid (Merck, 37 %)	1.01
Crystalline Fe oxides	CFeO <sub>x</sub>	0.5	0.2 M ammonium oxalate (Merck, 99 %) + 0.2 M oxalic acid (Merck, 99 %) + 0.1 M ascorbic acid (Merck, 99.7 %)	1.02

maximum value of the coefficient of determination ( $R^2$ ) and the minimum value of the standard error of estimate (SEE) (Nasrabadi et al., 2022).

## 2.6 Data analysis

An ANOVA test was utilized to assess treatment effects between the individual and combined biochar and silicon treatments. Additionally, a comparison of means was conducted using the MSTAT-C computer program, applying Duncan's test with a significance level of 5%. Figures were generated using Excel 2013 software. Pearson correlation coefficients among parameters in the dataset were determined using SPSS 12.0.

## 3 Results and discussion

### 3.1 Soil characteristics

The soil used in the study prior to experimental treatment exhibited a sandy loam texture and possessed alkaline properties with a significant calcium carbonate content (calcareous soil) but was not classified as saline (Table 2). The soil organic matter (OM) content and the cation exchange capacity (CEC) were extremely low (Table 2) compared with the values documented by Rassaei et al. (2020) for calcareous soils of Fars Province, southern Iran (OM: 1.20%–7.10%; CEC: 19.5–55.9 cmol<sub>(+)</sub> kg<sup>-1</sup>). The soils in Iran mainly originate from calcareous alluvium under xeric, ustic, or aridic moisture regimes and mesic, thermic, or hyperthermic temperature regimes. These soils have varied properties, such as calcium carbonate equivalent (1%–81%), clay content (1%–75%), EC (0.40–49.0 dS m<sup>-1</sup>), OM content (0.10%–21.5%), and gypsum content (0%–91%) (Ghiri et al., 2011). Furthermore, it should be noted that the concentration of available Ni extractable by DTPA in the soil was low (Table 2) compared with the mean value (0.60 mg Ni kg<sup>-1</sup>) reported by Jalali et al. (2022) for calcareous soils located in western Iran.

**Table 2.** Certain physicochemical attributes of the soil prior to cultivation.

Sand (%)	58.0
Silt (%)	30.0
Clay (%)	12.0
Soil textural class	Sandy loam
pH <sub>(s)</sub>	7.59
EC (dS m <sup>-1</sup> )	2.60
CCE (%)	55.0
OM (%)	0.50
CEC (cmol <sub>(+)</sub> kg <sup>-1</sup> )	11.7
Total Ni (mg kg <sup>-1</sup> )	28.0
Ni-DTPA (mg kg <sup>-1</sup> )	0.39

Notes: EC, electrical conductivity; CCE, calcium carbonate equivalent; OM, organic matter; CEC, cation exchange capacity.

### 3.2 Chemical characteristics of the biochars

As the pyrolysis temperature rose from 300 to 500 °C, the SM biochars demonstrated elevated pH and EC values, with the highest levels observed at the highest temperature (Table 3). The elevated levels of alkali salts, which are reflected in the high ash content (Table 3), are the contributing factor behind this observation in the SM biochars in comparison to the RH biochars. Plant-based biochars commonly exhibit reduced levels of dissolved solids in comparison to animal-based biochars (Sun et al., 2014). The SM300 biochar possessed the highest CEC value of 19.70 cmol<sub>(+)</sub> kg<sup>-1</sup>. The observed phenomenon may be attributed to the diminution of surface functional groups, namely, carboxyl and phenol, at elevated pyrolysis temperatures. These groups are predominantly responsible for facilitating the cation exchange capacity (CEC) of biochars (Tomczyk et al., 2020). As the pyrolysis temperature increased, there was an observed increase in the C content of the biochars as well as a corresponding decrease in the content of hydrogen, oxygen, and nitrogen (Table 3). The observed increase in the concentration of C as the pyrolysis temperature rises is consistent with a concomitant rise in the degree of carbonization. The observed

**Table 3.** Some physical and chemical properties of the biochars.

	SM300	SM500	RH300	RH500
pH (1 : 20)	9.96	11.0	9.00	10.3
EC (1 : 20) (dS m <sup>-1</sup> )	3.94	4.28	0.84	1.17
CEC (cmol <sub>c</sub> kg <sup>-1</sup> )	19.7	18.9	18.9	15.3
C (%)	25.4	31.8	45.0	50.0
H (%)	1.85	0.80	2.28	1.06
N (%)	2.10	1.57	1.30	1.10
Ni (mg kg <sup>-1</sup> )	3.00	15.4	Nd	Nd
Moisture content (%)	1.91	1.82	2.65	2.37
Ash content (%)	53.8	60.0	34.2	44.8
H : C mole ratio	0.87	0.30	0.60	0.25
O + S : C mole ratio	0.44	0.09	0.24	0.01

Notes: SM300, sheep manure biochar generated at 300 °C; SM500, sheep manure biochar generated at 500 °C; RH300, rice husk biochar produced at 300 °C; RH500, rice husk biochar produced at 500 °C; EC, electrical conductivity; CEC, cation exchange capacity; Nd, non-detectable.

reduction in the levels of H and O might be attributed to the occurrence of dehydration reactions, the decomposition of oxygenated bonds, and the liberation of low-molecular-weight byproducts rich in H and O, as recently noted by Zhao et al. (2017). Nitrogen compound volatilization explains the diminished N content of the biochars at elevated pyrolysis temperatures. The H : C and O : C ratios are significant indicators of the aromaticity and polarity of biochars; the lower the ratios the more condensed aromatic C the biochar contains (Chatterjee et al., 2020). The results shown in Table 3 indicate that the H : C and O : C mole ratios showed a gradual decrease as the pyrolysis temperature was increased, which can be interpreted as a sign of improved carbonization of the biochars (Zhao et al., 2017). The Ni content in the biochars derived from rice husk was below detection, whereas a limited quantity of Ni was detected in the biochars produced from sheep manure (Table 3).

### 3.3 Biochar analysis using FTIR and SEM

The FTIR spectra of the SM and RH biochars are shown in Fig. 2. The SM and RH biochars produced at 300 °C contained a higher content of carboxyl groups (1700 cm<sup>-1</sup>) (Keiluweit et al., 2010) than the biochars produced at 500 °C, which is in agreement with the O : C values of the biochars (Table 3). All of the biochars contained absorption bands associated with lignin (1430 cm<sup>-1</sup>) and cellulose (1030–1160 cm<sup>-1</sup>) (Keiluweit et al., 2010). The SM biochar contained more calcite than the RH biochar, as indicated by the greater intensity of calcite-characteristic peaks at 1432, 875, and 711 cm<sup>-1</sup> (Myszka et al., 2019) in the SM biochars (Fig. 2a). There was also evidence of the presence of Ca oxalate in the SM biochars, indicated by the characteristic peaks at 1618, 780, and 518 cm<sup>-1</sup> (Maruyama et al., 2023). All of the biochars contained silica, as indicated by the intense

silica absorption peaks at 1100, 800, and 470 cm<sup>-1</sup> (Zem-nukhova et al., 2015).

The SEM images of the SM and RH biochars are shown in Fig. 3. The morphology of the biochars became more rigid and porous at higher temperatures, as evidenced by the cell wall shrinkage attributed to the devolatilization of organic tissues (Claoston et al., 2014).

### 3.4 Nickel content in various soil chemical fractions after the application of Si levels and biochars

The interaction of treatments (biochars and Si levels) had a statistically significant effect ( $P < 0.01$ ) on the Ni concentration in all of the soil chemical fractions except for the Car fraction, whereas the main effects of the individual treatments (biochars and Si levels) on the Ni concentration in all of the soil chemical fractions were significant. The Ni concentration in the WsEx fraction was significantly reduced (by 14.8 %) by the application of Si levels from 6.07 to 5.17 mg Ni kg<sup>-1</sup> ( $S_0$  to  $S_2$ ) (Table 4). Among the biochar treatments, the greatest decrease in the Ni content (from 6.04 to 5.01 mg Ni kg<sup>-1</sup> by 17 %) in the WsEx fraction compared with the control was due to SM500, whereas the RH300 treatment had no significant effect (Table 4). The interaction effects of treatments indicated that the lowest Ni content in the WsEx fraction was due to the combined treatment of SM500 +  $S_2$  (4.04 mg Ni kg<sup>-1</sup> soil) (Table 4). The combined treatment of  $S_2$  and SM biochars had a strong synergistic effect on reducing the Ni content in the WsEx fraction (23 %–36 % reduction) compared with the sum of the treatments alone (13 %–15 % reduction) (Fig. 4), whereas this synergistic effect of the combined treatments was not evident for the RH biochars (Fig. 4). There was a negative correlation between the Ni content in the WsEx fraction and soil pH ( $r = -0.66$ ,  $P < 0.01$ ), indicating that the reduction in the Ni content in the WsEx fraction was strongly linked to the increase in soil pH due to the amendments (Supplement). Previous studies have also shown that the application of biochars and silicates result in increases in soil pH, thereby reducing the bioavailability of PTEs and their conveyance to plant roots (Shen et al., 2020; Ma et al., 2021). Among the applied biochars, the maximum pH (Table 3), ash content (Table 3), and calcite (lime) content (Fig. 2) were attributed to the SM500 biochar. Therefore, the combined SM500 +  $S_2$  treatment was most effective at reducing the Ni content in the WsEx fraction, likely due to the higher alkalinity and ash content of SM500 promoting Ni precipitation and adsorption (Sachdeva et al., 2023). The increase in soil pH due to Na metasilicate also likely enhanced the precipitation of Ni in the forms of Ni silicate and hydroxide. Addition of Si in the form of Na metasilicate increases soil pH due to the hydrolysis of the silicate anion in soil solution, which generates hydroxyl ions (Ma et al., 2021).

The reduced effectiveness of biochars produced at 300 °C (compared with those produced at 500 °C) with respect to

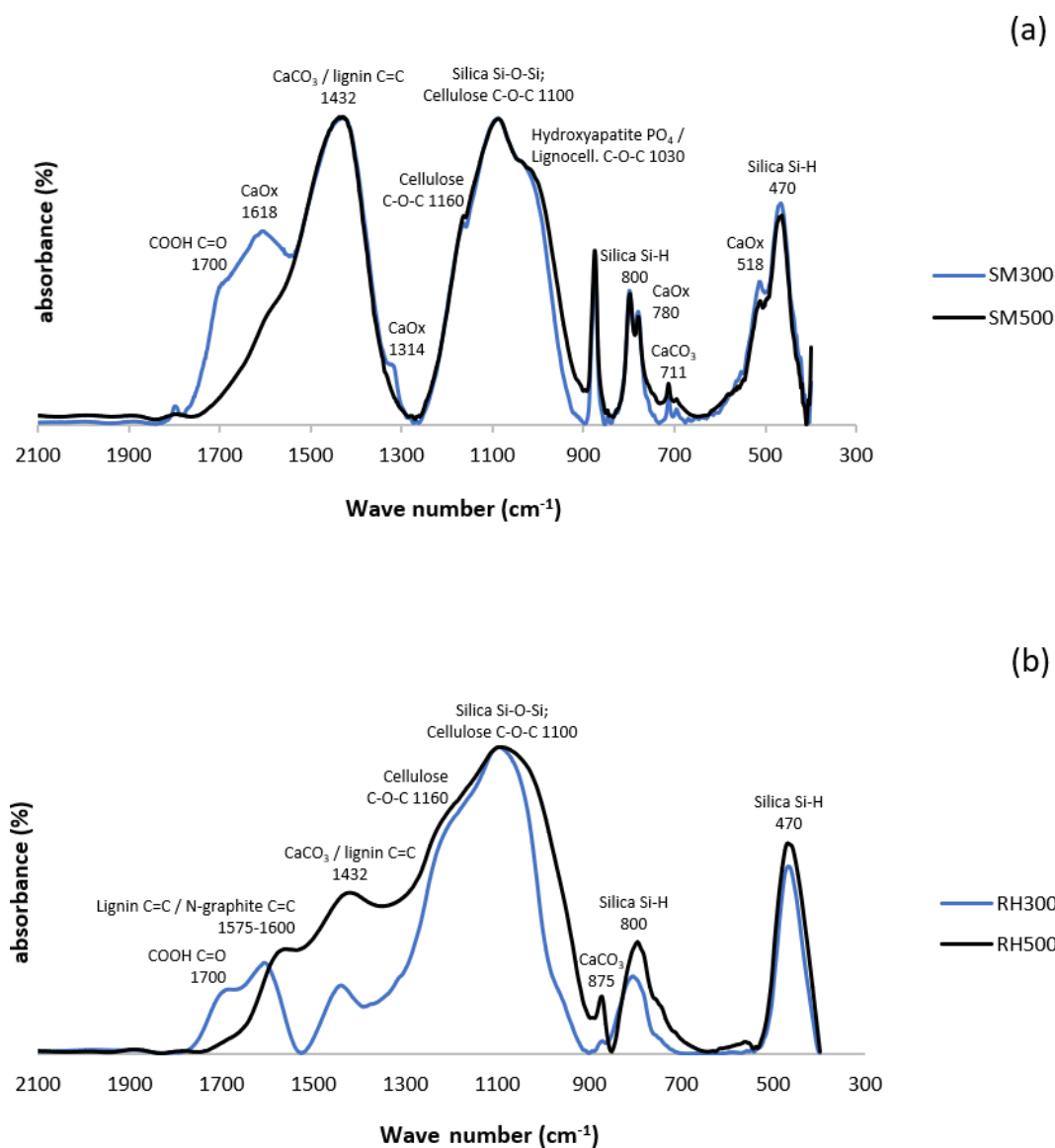


**Figure 2.** FTIR spectra the biochars in the wave number range of 400–2000  $\text{cm}^{-1}$ . Notes: SM300, sheep manure biochar produced at 300 °C; SM500, sheep manure biochar produced at 500 °C; RH300, rice husk biochar produced at 300 °C; RH500, rice husk biochar produced at 500 °C.

decreasing the Ni content in the WsEx fraction could also be attributed to the lower rates of microbial oxidation and mineralization of RH500 and SM500, as reflected in their greater environmental stability (indicated by the lower H : C mole ratio values) (Table 3). Consequently, biochar produced at 500 °C may not provide sufficient acidic carboxyl functional groups to the soil to stimulate soil organic matter (SOM) decomposition, leading to a greater increase in soil pH (Sun et al., 2023). According to Zhu et al. (2015), the addition of biochar based on wine lees (material from a wine processing factory) to a heavy-metal-contaminated soil (at levels of 0.5 % and 1 %  $w/w$ ) resulted in an increase in soil pH and a decrease in the Ni content in the WsEx fraction.

As there was no significant interaction effect between biochar type and Si levels on the Ni concentration in the Car fraction, only the significant individual main effects of biochar and Si levels are shown in Fig. 5. Changing the Si application levels from  $S_0$  to  $S_2$  significantly decreased the Ni content in the Car fraction by 11.7 % (from 15.2 to 13.5  $\text{mg Ni kg}^{-1}$  soil) (Fig. 5). The decrease in the concentration of Ni in the Car form with an increase in the Si levels could potentially be explained by the competition between silicate ( $\text{SiO}_4^{4-}$ ) and carbonate ions for binding with  $\text{Ni}^{2+}$  ions in the soil solution (Sparks et al., 2022). The SM biochars had no significant effect on the Ni concentration in the Car fraction, whereas the addition of RH biochars led to

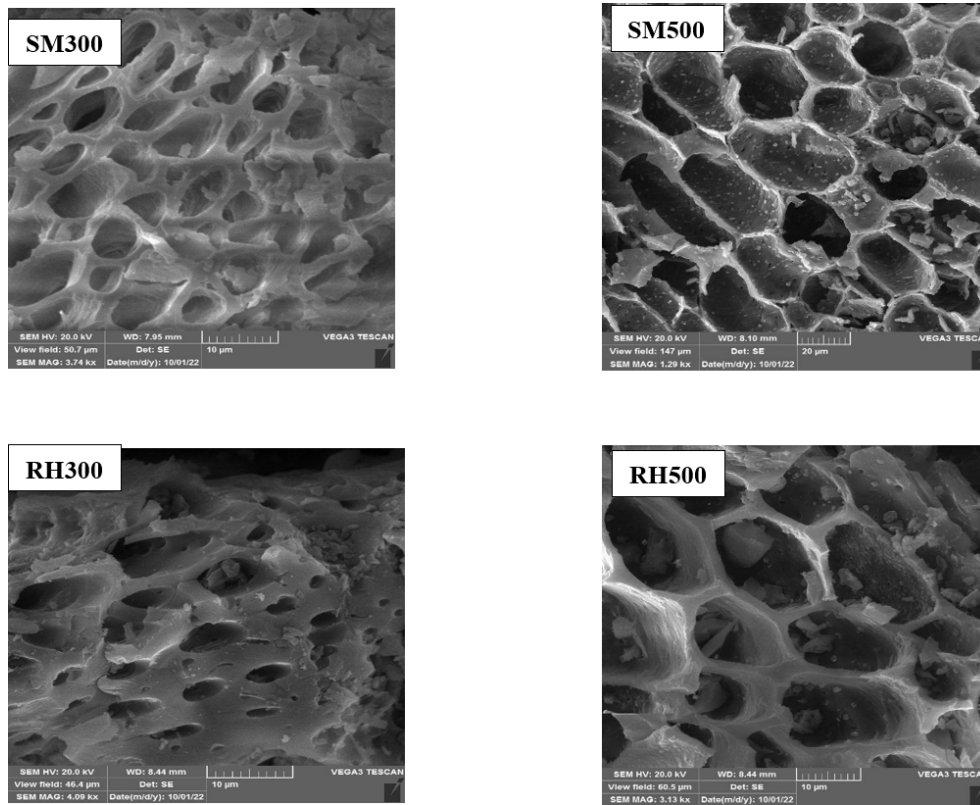


**Figure 3.** SEM images of the biochars. Notes: SM300, sheep manure biochar produced at 300 °C; SM500, sheep manure biochar produced at 500 °C; RH300, rice husk biochar produced at 300 °C; RH500, rice husk biochar produced at 500 °C.

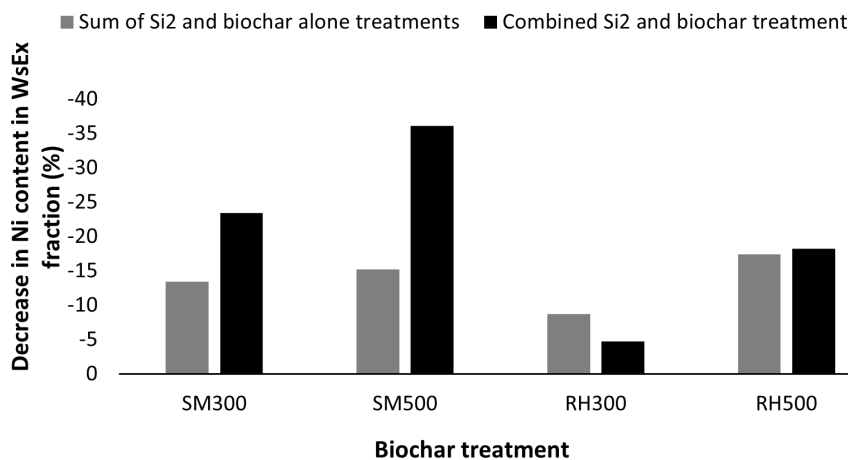


**Figure 4.** Comparison of the effect of the sum of the Si<sub>2</sub> and biochar alone treatment versus the combined Si<sub>2</sub> and biochar treatments on the decrease in the Ni content in the WsEx fraction. Notes: SM300, sheep manure biochar produced at 300 °C; SM500, sheep manure biochar produced at 500 °C; RH300, rice husk biochar produced at 300 °C; RH500, rice husk biochar produced at 500 °C.

a significant increase in the Ni concentration in this fraction (Fig. 5). Ippolito et al. (2017) found that the addition of two biochars, pine (*Pinus contorta*) and tamarisk (*Tamarix* spp.), to a soil contaminated by mining activities caused a significant increase in the soil Cd content bound to carbonates. They concluded that the reduction in Cd bioavailability may

have been due to the ability of biochar to raise soil pH levels and induce the precipitation of CdCO<sub>3</sub>. Similarly, Yuan et al. (2011) proposed that the decrease in the bioavailability of PTEs in soil amended by biochars derived from different crop residues might have been caused by the creation of metal-carbonate species and carbonate-surface functional

**Table 4.** Effects of biochars and Si application levels on the Ni concentration ( $\text{mg kg}^{-1}$ ) in different soil chemical fractions after corn cultivation.

	C	SM300	SM500	RH300	RH500	Mean
	WsEx					
$S_0$	6.32 a	6.02 a–c	5.91 bc	6.31 a	5.77 c	<b>6.07 A</b>
$S_1$	6.03 a–c	5.37 d	5.09 de	6.25 ab	5.28 d	<b>5.60 B</b>
$S_2$	5.77 c	4.84 e	4.04 f	6.02 a–c	5.17 de	<b>5.17 C</b>
Mean	<b>6.04 A</b>	<b>5.41 B</b>	<b>5.01 C</b>	<b>6.20 A</b>	<b>5.41 B</b>	
	OM					
$S_0$	9.72 a	10.6 a	8.04 d–f	10.0 a	9.02 b	<b>9.40 A</b>
$S_1$	9.60 a	9.75 a	7.16 g	8.62 b–d	8.70 bc	<b>8.76 B</b>
$S_2$	8.11 c–f	7.94 ef	7.12 g	8.30 c–e	7.63 fg	<b>7.82 C</b>
Mean	<b>9.14 A</b>	<b>9.28 A</b>	<b>7.44 C</b>	<b>8.99 A</b>	<b>8.44 B</b>	
	$\text{MnO}_x$					
$S_0$	11.6 a	3.77 kl	5.99 f	4.69 gh	9.71 c	<b>7.15 A</b>
$S_1$	10.3 b	3.50 l	5.00 g	4.57 hi	8.93 d	<b>6.48 B</b>
$S_2$	10.3 b	2.98 m	4.28 ij	3.96 jk	7.94 e	<b>5.89 C</b>
Mean	<b>10.7 A</b>	<b>3.42 E</b>	<b>5.09 C</b>	<b>4.41 D</b>	<b>8.86 B</b>	
	$\text{AFeO}_x$					
$S_0$	11.1 ef	10.4 g	11.8 d	11.0 fg	11.7 de	<b>11.2 C</b>
$S_1$	12.2 b–d	10.7 fg	12.0 cd	12.2 b–d	12.7 bc	<b>12.0 B</b>
$S_2$	12.8 b	12.2 b–d	12.2 b–d	12.3 b–d	14.2 a	<b>12.7 A</b>
Mean	<b>12.1 B</b>	<b>11.1 C</b>	<b>12.0 B</b>	<b>11.8 B</b>	<b>12.9 A</b>	
	$\text{CFeO}_x$					
$S_0$	77.3 f	78.0 f	84.0 cd	84.7 cd	79.6 ef	<b>80.7 C</b>
$S_1$	77.9 f	82.2 de	86.3 bc	85.1 b–d	83.6 cd	<b>83.0 B</b>
$S_2$	79.9 ef	85.5 bc	87.9 ab	85.7 bc	90.4 a	<b>85.9 A</b>
Mean	<b>78.4 C</b>	<b>81.9 B</b>	<b>86.0 A</b>	<b>85.2 A</b>	<b>84.5 A</b>	
	Res					
$S_0$	200 c–e	207 a	200 c–e	196 f	198 d–f	<b>200 A</b>
$S_1$	200 c–e	204 b	200 c–e	197 ef	195 f	<b>199 A</b>
$S_2$	200 cd	204 b	201 c	199 c–e	190 g	<b>199 A</b>
Mean	<b>200 B</b>	<b>205 A</b>	<b>200 B</b>	<b>198 B</b>	<b>195 BC</b>	

Notes: C, control; SM300, sheep manure biochar produced at 300 °C; SM500, sheep manure biochar produced at 500 °C; RH300, rice husk biochar produced at 300 °C; RH500, rice husk biochar produced at 500 °C;  $S_0$ , without Si addition;  $S_1$ , application of 250  $\text{mg Si kg}^{-1}$  soil;  $S_2$ , application of 500  $\text{mg Si kg}^{-1}$  soil; WsEx, water-soluble and exchangeable fraction; OM, organic fraction;  $\text{MnO}_x$ , bound to manganese oxides;  $\text{AFeO}_x$ , bound to amorphous iron oxides;  $\text{CFeO}_x$ , bound to crystalline iron oxides; Res, residual fraction. Numbers followed by the same letters in each column and row in each section are not significantly ( $P < 0.05$ ) different. The main effects of treatments are shown using bold font.

group reactions, which could function as a mechanism for sequestration.

The biochars produced at 300 °C had no significant effect on the Ni content in the OM fraction compared to the control, whereas the biochars generated at 500 °C significantly decreased it (Table 4). The greatest reduction in the Ni content in the OM fraction (18.6 %) was found to be in that which underwent the SM500 treatment. Lu et al. (2017) explored how the application of bamboo and rice straw biochars with vary-

ing mesh sizes (0.25 and 1 mm) and at three different levels (0, 1, and 5 %  $w/w$ ) affected the distribution of Cd in a contaminated sandy loam soil, using the BCR (Bureau Communautaire de Référence) sequential extraction method. In contrast to the present study, they reported that the biochars increased the concentration of Cd in the OM fraction, and this was closely related to the increase in Cd immobilization. In another study, the application of sheep manure biochar produced at 500 °C at a rate of 3wt % to a Cd-contaminated cal-

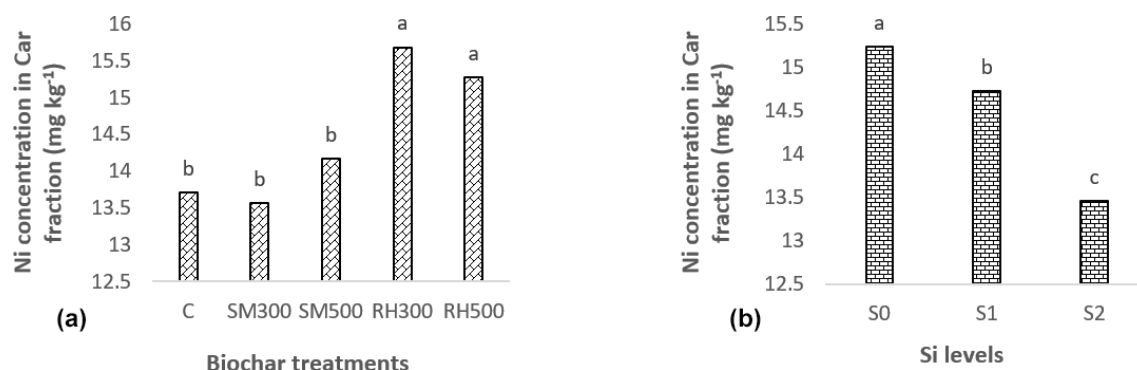


**Figure 5.** Main effects of the (a) biochar type and (b) Si application levels on the Ni concentration ( $\text{mg kg}^{-1}$ ) in the Car fraction after corn cultivation. Notes: C, control; SM300, sheep manure biochar produced at 300 °C; SM500, sheep manure biochar produced at 500 °C; RH300, rice husk biochar produced at 300 °C; RH500, rice husk biochar produced at 500 °C; S<sub>0</sub>, without Si addition; S<sub>1</sub>, application of 250  $\text{mg Si kg}^{-1}$  soil; S<sub>2</sub>, application of 500  $\text{mg Si kg}^{-1}$  soil. Numbers followed by the same letters in each section are not significantly ( $P < 0.05$ ) different.

careous soil resulted in a significant increase in the Cd content in the OM fraction, whereas the addition of other biochar treatments (wheat straw, corn straw, rice husk, and licorice root pulp) caused a significant decrease in the concentration of Cd in the OM fraction when compared with the control soil (Boostani et al., 2018). In the study conducted by Boostani et al. (2018), the reduction in the Cd concentration in the OM fraction as a result of the application of rice husk biochar is in line with our findings, however; the increase in the Cd content in the OM form with the addition of sheep manure biochar is in contrast with the result of the present study. These observations indicate that, in addition to the characteristics of biochar and the level of its application (Lu et al., 2017), soil characteristics (calcium carbonate percentage, soil texture, etc.) and the type of heavy metal can also have a substantial role in the binding of PTEs to soil organic matter. Changing the Si levels from S<sub>0</sub> to S<sub>2</sub> reduced the Ni concentration in the OM fraction by 16.8 % (Table 4). Ma et al. (2021) reported that the application of Si to cultivated soils significantly reduced the soil OM content, which could explain why the Ni concentration in the OM fraction was reduced in the present study. They indicated that Si facilitates the decomposition of organic matter by enhancing soil pH. In this study, the interaction effects of biochars and Si levels showed that the lowest Ni content in the OM fraction was due to the combined treatment of SM500 + S<sub>2</sub> (7.12  $\text{mg Ni kg}^{-1}$  soil), which was equal to a 26.7 % decrease compared with the control (CS<sub>0</sub>) (9.72  $\text{mg Ni kg}^{-1}$  soil) (Table 4).

All of the biochar treatments caused a significant decrease in the Ni content in the MnO<sub>x</sub> fraction compared with the control, with the greatest reduction (52.6 %) caused by the SM300 treatment (Table 4). The lower-temperature biochars were more effective than the higher-temperature biochars with respect to decreasing the Ni content in the MnO<sub>x</sub> fraction (Table 4). In agreement with the present study, Boostani et al. (2023c) observed that biochars produced from cow ma-

nure, municipal solid waste, and licorice root pulp at a lower pyrolysis temperature (300 °C) decreased the Ni content in the MnO<sub>x</sub> fraction to a greater extent than those prepared at a higher temperature (600 °C). Hydrophobicity of biochar is decreased with increasing pyrolysis temperature (Kameyama et al., 2019). It is well known that, at the same soil water content, the water content of soil pores treated with biochars produced at lower pyrolysis temperatures is higher due to the lower absorption of water by the biochars. Therefore, in soils with high-soil-pore-water-content and low-oxygen conditions, the concentration of MnO<sub>x</sub> is decreased due to chemical reduction, while the Mn concentration in the exchangeable and water-soluble fraction is concomitantly increased (Sparrow and Uren, 2014). Furthermore, increasing the Si application levels from S<sub>0</sub> to S<sub>2</sub> significantly decreased the Ni content in the MnO<sub>x</sub> fraction by 17.6 % (Table 4). Compared with the control, which had the highest concentration of Ni in the MnO<sub>x</sub> fraction (11.58  $\text{mg Ni kg}^{-1}$  soil), the greatest interactive effect in the reduction of this fraction (3.8 fold) was related to the combined SM300 + S<sub>2</sub> (2.98  $\text{mg Ni kg}^{-1}$  soil) treatment (Table 4). The concentration of Ni bound to the AFeO<sub>x</sub> and CF<sub>2</sub>O<sub>x</sub> fractions was significantly increased by the application of Si levels from S<sub>0</sub> to S<sub>2</sub>, by 13.6 % and 6.5 %, respectively (Table 4). Belton et al. (2012) demonstrated that exogenous silicon application resulted in the attachment of silicate to the surface of iron oxide in the form of a polymer. Following the complexation of ferrosilicon, a significant number of negatively charged functional groups, including silanol, were formed. These groups provided numerous adsorption sites for PTEs, ultimately reducing their bioavailability (Belton et al., 2012). In general, all of the biochars caused a significant increase in the Ni content in the form of CF<sub>2</sub>O<sub>x</sub>, and there were no significant differences among the SM500, RH300, and RH500 treatments (Table 4). However, only the RH500 treatment increased the Ni concentration in the AFeO<sub>x</sub> fraction compared with the control

(Table 4). Among all of the biochars, only the SM300 treatment resulted in a significant increase in the Ni concentration in the Res fraction compared with the control (Table 4). The main (mean) effects of Si application showed that increasing the Si levels from  $S_0$  to  $S_2$  had no statistically significant effect on the Ni content in the Res fraction (Table 4).

Mailakeba and Bk (2021) studied the addition of kunai grass biochar (0.75 %) to a soil with different Ni contamination levels (0, 56, 100, and 180 mg Ni kg<sup>-1</sup> soil). They found that the application of the grass biochar increased the Ni content in the Res fraction and reduced Ni in the other fractions in the soil. In another study, Boostani et al. (2023c) demonstrated that the application of biochars – cow manure, municipal compost, and licorice root pulp, each at 3 % (*w/w*) – to a Ni-contaminated soil increased the Ni concentration in the OM and Res fractions and decreased the Ni content in the WsEx, Car, and Fe/Mn oxide fractions. In contrast, Boostani et al. (2023b) found that the application of manure and compost biochars (3 % *w/w*) to Pb-contaminated soil did not significantly affect the Pb content in the Res fraction but did decrease the WsEx fraction. Therefore, it seems that the effect of biochars on the changes in the chemical fractions of PTEs in soil depends on the raw materials and production conditions of the biochar, the soil application levels, the type of PTEs, the degree of soil contamination with PTEs, the selection of the sequential extraction procedure, and the soil properties (Mailakeba and Bk, 2021; Boostani et al., 2023b, a, 2021).

In summary, the application of biochars in the present study resulted in the transfer of Ni in soil from more bioavailable and mobile fractions (WsEx, MnO<sub>x</sub>, and OM) to other stable fractions (AFeO<sub>x</sub> and CFeO<sub>x</sub>). These changes were more evident in the WsEx fraction when SM biochars were applied in conjunction with Si (23 %–36 % reduction in the Ni content in the WsEx fraction compared with 13 %–15 % when applied alone), indicating that the simultaneous application of these two substances is much more effective than applying them separately.

### 3.5 Ni concentration in corn (*Zea mays* L.) shoots as affected by treatments

The main effects of biochars, Si application levels, and their interactive effects were statistically significant ( $P < 0.01$ ) on the Ni concentration in corn shoots. The main (mean) effects of Si application levels showed that changing the Si levels from  $S_0$  to  $S_2$  resulted in a 32 % decrease in the Ni concentration in shoots, from 8.56 mg Ni kg<sup>-1</sup> dry matter (DM) to 5.82 mg Ni kg<sup>-1</sup> DM (Table 5). In addition, the Ni concentration in shoots was significantly decreased by the application of all of the biochar treatments compared with the control (with no biochar addition) (Table 5). The interactive effects of treatments indicated that the lowest Ni concentration in shoots was observed in the combined treatment of SM500 +  $S_2$  (4.45 mg Ni kg<sup>-1</sup> DM), which showed a

57.2 % decrease compared with the control (CS<sub>0</sub>: without Si and biochar addition) (10.4 mg Ni kg<sup>-1</sup> DM) (Table 5). The Ni content in shoots had a significant and positive correlation with the Ni content in the WsEx fraction ( $r = +0.62$ ,  $P < 0.01$ ), while there was a significant and negative correlation between the soil pH ( $r = -0.60$ ,  $P < 0.01$ ) and Ni content in the CFeO<sub>x</sub> fraction ( $r = -0.50$ ,  $P < 0.01$ ) (Supplement). This indicates that the application of Si and biochar can reduce the Ni content in shoots by increasing soil pH and, as a result, reducing the amount of Ni in the fraction of WsEx and increasing the Ni content attached to the CFeO<sub>x</sub> fraction. Boostani et al. (2019a) reported a significant reduction in the concentration of Ni in spinach (*Spinacia oleracea* L.) shoots due to the application of rice husk and licorice root pulp biochars (2.5 % *w/w*) in a Ni-contaminated calcareous soil. Additionally, they reported that the biochars produced at 350 °C were more effective at reducing crop Ni uptake and promoting plant growth than the biochars produced at 550 °C. The most significant factors that contribute to the uptake reduction of PTEs by plants in contaminated soils that have been amended with biochars include the adsorption of heavy metals by surface functional groups, increased soil pH, reducing the mobility of PTEs by changing soil redox conditions, improved physical and biological properties of the soil, changes in the activity levels of antioxidant enzymes, and a decrease in the transfer of PTEs to the plant shoots (Zeng et al., 2018; Rizwan et al., 2016). Several studies have investigated the effect of Si application on Ni concentration in shoots and other heavy metals in various plant species. Khaliq et al. (2016) observed a notable increase in the Ni concentration and accumulation within the leaf, stem, and roots of cotton after Ni application, whereas Si application was observed to induce a significant reduction in Ni concentrations across these respective plant components. In another study, Maryam et al. (2024) concluded that the addition of Si caused an increase in the growth indices of maize by reducing the Pb concentration in shoots. One possible explanation for the reduction in the Ni concentration in shoots is that Si can compete with Ni for uptake by plant roots. Silicon has a similar ionic radius to Ni, which means that it can occupy the same binding sites on root cell membranes and reduce the uptake of Ni. Additionally, Si can induce the expression of genes that are involved in Ni transport and homeostasis, which may contribute to the reduced Ni concentration in shoots (Hossain et al., 2012; Liang et al., 2005).

### 3.6 Ni desorption in soil as affected by Si application levels and biochars

The cumulative Ni desorption (extracted by DTPA) values in the soil as a function of time are shown in Fig. 6. The release of Ni from the soil initially proceeded at a much higher rate during the first hour; it then proceeded at a much slower rate during the next 24 h, as illustrated by the trend line in Fig. 6. This two-stage process of releasing heavy metals from soil

**Table 5.** Ni concentration ( $\text{mg Ni kg}^{-1}$  DM) in corn shoots as affected by biochars and Si application levels.

	C	SM300	SM500	RH300	RH500	Mean
$S_0$	10.4 a	7.35 bc	9.85 a	7.55 bc	7.65 b	<b>8.56 A</b>
$S_1$	7.65 b	6.90 bc	6.60 cd	7.05 bc	7.35 bc	<b>7.11 B</b>
$S_2$	7.20 bc	5.05 ef	4.45 f	5.80 de	6.60 cd	<b>5.82 C</b>
Mean	<b>8.41 A</b>	<b>6.43 C</b>	<b>6.96 BC</b>	<b>6.80 BC</b>	<b>7.20 B</b>	

Notes: C, control; SM300, sheep manure biochar generated at 300 °C; SM500, sheep manure biochar generated at 500 °C; RH300, rice husk biochar produced at 300 °C; RH500, rice husk biochar produced at 500 °C;  $S_0$ , without Si application;  $S_1$ , addition of 250  $\text{mg Si kg}^{-1}$  soil;  $S_2$ , addition of 500  $\text{mg Si kg}^{-1}$  soil. Numbers followed by the same letters in each section are not significantly ( $P < 0.05$ ) different. The main effects of treatments are shown using bold font.

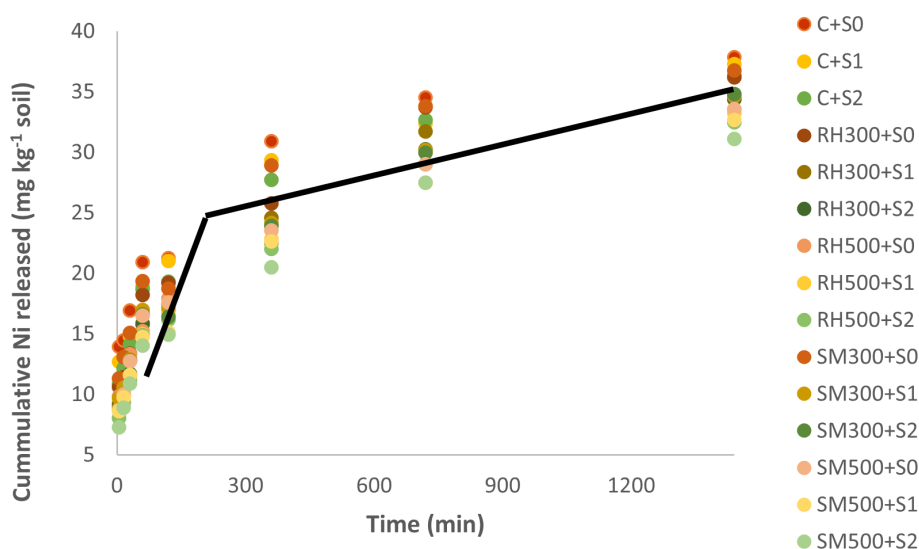


**Figure 6.** Cumulative Ni desorption (extracted by DTPA) ( $\text{mg kg}^{-1}$ ) in the soil as affected by different treatments. Notes: C, control; SM300, sheep manure biochar produced at 300 °C; SM500, sheep manure biochar produced at 500 °C; RH300, rice husk biochar produced at 300 °C; RH500, rice husk biochar produced at 500 °C;  $S_0$ , without Si addition;  $S_1$ , application of 250  $\text{mg Si kg}^{-1}$  soil;  $S_2$ , application of 500  $\text{mg Si kg}^{-1}$  soil.

has also been reported by other researchers (Sajadi Tabar and Jalali, 2013; Boostani et al., 2023b). It is likely that the first stage of Ni release is related to forms that are less strongly attached to soil particles, including  $\text{WsEx}$  and  $\text{Car}$ , while the second stage of Ni desorption is likely from soil chemical fractions with less bioavailability, such as  $\text{FeO}_x$  and  $\text{Res}$  (Saffari et al., 2015). In general, the amount of Ni desorption in the soil was reduced by the addition of biochars and Si levels (Fig. 6). In addition, the effects of biochars produced at the higher pyrolysis temperature (500 °C) on reducing Ni release was more than those generated at the lower pyrolysis temperature (300 °C) in the soil. The highest amount of Ni release was due to the control ( $\text{CS}_0$ : without biochar and Si application) ( $37.84 \text{ mg Ni kg}^{-1}$  soil), whereas the lowest was observed in the combined application of SM500 and  $S_2$  ( $31.13 \text{ mg Ni kg}^{-1}$  soil) treatment.

### 3.7 Fitting of Ni release data to kinetics models

The Ni release data during 24 h for all of the biochar and Si treatments were evaluated by seven different kinetics models (Table 6). The effectiveness of the various kinetics models to describe the observed Ni desorption in the soil was analysed by considering the coefficient of determination ( $R^2$ ) and standard error of estimate (SEE) values. The highest value of the  $R^2$  and the lowest value of the SEE were set as the criteria. As seen in Table 6, the order kinetics models did not adequately describe Ni release in the soil, and the value of the  $R^2$  decreased with an increase in the order of the kinetics model (from zero to third order). This has also been found by other researchers for the release of heavy metals from soil (Boostani et al., 2019b; Ghasemi-Fasaei et al., 2006). In contrast, the non-order kinetics models, including the power function, parabolic diffusion, and simple Elovich models, acceptably described the Ni release in the soil amended with various treatments (Table 6). Among them, the power function model

**Table 6.** The range of coefficient of determination ( $R^2$ ) and standard error of estimate (SEE) values for the kinetics models applied to all of the soil treatments.

Kinetics models	$R^2$		SEE	
	Range	Mean	Range	Mean
Zero order	0.79–0.87	0.80	3.36–4.67	3.67
First order	0.69–0.75	0.75	0.22–0.29	0.25
Second order	0.53–0.61	0.52	$(1.10–2.60) \times 10^{-2}$	$1.80 \times 10^{-2}$
Third order	0.39–0.51	0.41	$(1.30–5.20) \times 10^{-3}$	$3.00 \times 10^{-3}$
Parabolic diffusion	0.94–0.98	0.96	1.26–2.44	1.85
Power function	0.97–0.99	0.98	0.05–0.06	0.05
Simple Elovich	0.92–0.97	0.95	2.04–2.78	2.50

**Table 7.** The coefficients of the power function model as affected by biochars and Si application levels in a Ni-polluted calcareous soil after corn cultivation.

	C	a (mg Ni kg <sup>-1</sup> h <sup>-1</sup> ) <sup>b</sup>				Mean
		SM300	SM500	RH300	RH500	
$S_0$	9.15 a	7.39 c	5.56 gh	6.49 e	5.95 f	<b>6.91 A</b>
$S_1$	7.92 b	6.01 f	5.23 i	5.66 g	5.21 i	<b>6.00 B</b>
$S_2$	6.90 d	5.39 hi	4.52 k	5.22 i	4.84 j	<b>5.38 C</b>
Mean	<b>7.99 A</b>	<b>6.27 B</b>	<b>5.11 E</b>	<b>5.80 C</b>	<b>5.34 D</b>	
		b (mg Ni kg <sup>-1</sup> ) <sup>-1</sup>				
$S_0$	0.20 g	0.22 e	0.25 b	0.24 c	0.24 c	<b>0.23 C</b>
$S_1$	0.21 f	0.24 c	0.25 b	0.25 b	0.25 b	<b>0.24 B</b>
$S_2$	0.23 d	0.25 b	0.26 a	0.26 a	0.26 a	<b>0.25 A</b>
Mean	<b>0.21 C</b>	<b>0.24 B</b>	<b>0.25 A</b>	<b>0.25 A</b>	<b>0.25 A</b>	
		ab				
$S_0$	1.79 a	1.68 c	1.37 h	1.54 e	1.41 g	<b>1.55 A</b>
$S_1$	1.69 b	1.43 f	1.29 k	1.41 fg	1.32 j	<b>1.42 B</b>
$S_2$	1.59 d	1.37 h	1.19 m	1.34 i	1.27 l	<b>1.35 C</b>
Mean	<b>1.69 A</b>	<b>1.48 B</b>	<b>1.28 E</b>	<b>1.43 C</b>	<b>1.33 D</b>	

Notes: C, control; SM300, sheep manure biochar produced at 300 °C; SM500, sheep manure biochar produced at 500 °C; RH300, rice husk biochar produced at 300 °C; RH500, rice husk biochar produced at 500 °C;  $S_0$ , without Si addition;  $S_1$ , application of 250 mg Si kg<sup>-1</sup> soil;  $S_2$ , application of 500 mg Si kg<sup>-1</sup> soil. Numbers followed by the same letters in each column and row in each section are not significantly ( $P < 0.05$ ) different. The main effects of treatments are shown using bold font.

was the best, according to the highest value of  $R^2$  (0.98) and the lowest value of SEE (0.055). Boostani et al. (2018) also reported that the power function was the best kinetics model to describe Cd desorption in a Cd-contaminated soil treated with biochars and zeolite.

### 3.8 Using the parameters of the power function model to investigate the effect of treatments on Ni desorption in soil

As the power function model ( $q = at^b$ ) described the Ni release data the best, its parameters ( $a$  and  $b$ ) were used to investigate the effect of biochar application and Si levels on the release of Ni in the Ni-contaminated soil (Table 7). The

main effects of biochars and Si levels and their interactions on the  $a$  and  $b$  parameters were significant ( $P < 0.01$ ). As Dang et al. (1994) reported, in this kinetics model, a decrease in parameter  $a$  and an increase in parameter  $b$  indicate a decrease in the rate of heavy-metal desorption from the soil. The main effects of the treatments showed that the addition of all four biochars caused a significant decrease in the  $a$  parameter compared with the control, whereas the  $b$  parameter was significantly increased (Table 7). The same trend was observed for all of the Si treatment levels (Table 7). Therefore, it can be concluded that the use of all of the biochars and Si levels caused a decrease in the rate of Ni release in the Ni-contaminated soil. Generally, there was a greater decrease

**Table 8.** The Pearson correlation coefficients ( $r$ ) among the power function model parameters ( $a$ ,  $b$ ,  $ab$ ) with the Ni content in soil chemical fractions, the Ni concentration in corn shoots, and soil pH.

	WsEx	Car	OM	MnO <sub>x</sub>	AFeO <sub>x</sub>	CFeO <sub>x</sub>	Res	Ni content in shoots	Soil pH
$a$	0.63*	0.02 <sup>ns</sup>	0.70*	0.53*	-0.44*	-0.80*	0.27 <sup>ns</sup>	0.62*	-0.52*
$b$	-0.59*	0.03 <sup>ns</sup>	-0.68*	-0.54*	0.46*	0.83*	-0.28 <sup>ns</sup>	-0.63*	0.51*
$ab$	0.68*	0.04 <sup>ns</sup>	0.74*	0.46*	-0.46*	-0.80*	0.29 <sup>ns</sup>	0.06*	-0.51*

Notes: WsEx, water-soluble and exchangeable fraction; OM, organic fraction; MnO<sub>x</sub>, bound to manganese oxides; AFeO<sub>x</sub>, bound to amorphous iron oxides; CFeO<sub>x</sub>, bound to crystalline iron oxides; Res, residual fraction.

\*\* and <sup>ns</sup> indicate significance at the 0.01 probability level and non-significant, respectively.

in Ni desorption in biochar treatments prepared at the higher temperature (Table 7). The interactive effects indicate that the most effective combined treatment with respect to reducing the rate of Ni release in the soil was SM500 + S<sub>2</sub> which had the lowest value of parameter  $a$  (4.52) and the highest value of parameter  $b$  (0.26) among the treatments.

If it is differentiated from the power function equation ( $q = at^b$ ) with respect to time ( $t$ ) ( $dq/dt = abt^{b-1}$ ), when  $t = 1$  and  $s = 0$ , the ratio of  $dq/dt$  becomes  $ab$ . This parameter indicates the amount of heavy-metal desorption at the initial time (Dalal, 1985). The  $ab$  parameter was affected by the application of Si levels and biochars; thus, this parameter was significantly decreased compared with the control with the addition of all of the biochars (12.4 %, 24.2 %, 15.4 %, and 21.3 % for the SM300, SM500, RH300, and RH500 treatments, respectively) and Si application levels (13 % from S<sub>0</sub> to S<sub>2</sub>) (Table 7). This finding also confirmed the effect of applied treatments with respect to reducing the amount of Ni release. The greatest reduction was observed in the combined treatment of SM500 + S<sub>2</sub> by 33.5 % compared with the control (Table 7).

The correlation between the parameters of the fitted power function model with the Ni content in various soil chemical fractions, the Ni concentration in corn shoots, and soil pH are shown in Table 8. The  $a$  and  $ab$  parameters had a positive correlation with the Ni content in the WsEx, OM, and MnO<sub>x</sub> fractions, whereas these parameters had a negative correlation with the Ni content in the AFeO<sub>x</sub> and CFeO<sub>x</sub> fractions. This trend was inverse for the  $b$  parameter of the power function model. These correlations verified that the application of Si and biochar to the Ni-contaminated calcareous soil led to a decrease in the rate and amount of Ni release by reducing the Ni concentration in chemical forms with higher bioavailability, including WsEx, OM, and MnO<sub>x</sub>. Furthermore, the  $a$  and  $ab$  parameters were negatively correlated with soil pH, whereas there were positive correlations between these parameters and the Ni concentration in shoots (Table 8). These findings once again confirmed that the increase in soil pH due to the application of Si and biochar can cause a decrease in the bioavailability of Ni in the soil and, as a result, a decrease in the concentration of Ni in aerial parts of the plant.

## 4 Conclusions

The application of biochars and Si in the present study resulted in the transfer of Ni in soil from more bioavailable and mobile fractions (WsEx, MnO<sub>x</sub>, and OM) to more stable forms (AFeO<sub>x</sub> and CFeO<sub>x</sub>). These changes were particularly evident in the WsEx fraction when SM biochars were applied in conjunction with silicon, indicating a strong synergistic effect related to a soil pH increase. The application of all biochars and Si decreased the DPTA-extractable Ni release in the soil, which was most strongly associated with the increase in the Ni content in the CFeO<sub>x</sub> fraction. The application of all of the biochars and Si decreased corn Ni uptake, with the combined SM500 + S<sub>2</sub> being the most effective. The decrease in corn Ni uptake was correlated with a decrease in the Ni content in the WsEx fraction and an increase in the CFeO<sub>x</sub> fraction. SM500 was likely the most effective biochar due to its higher alkalinity and ash content and its lower acidic functional group content, which enhances Ni sorption reactions with Si. Future research is needed to better understand the mechanisms underlying the interaction effects of Si and biochar application on the distribution of Ni in different soil chemical fractions and to optimize Si application strategies for sustainable Ni management in agricultural and natural ecosystems. It is suggested that the interactive effects of Si and biochar on the Ni content in soil chemical fractions and its release in aged Ni-contaminated soils should also be investigated and compared, as this study was limited to a recently Ni-contaminated soil.

**Data availability.** The data generated in this study are available from the corresponding authors upon reasonable request.

**Supplement.** The supplement related to this article is available online at: <https://doi.org/10.5194/soil-10-487-2024-supplement>.

**Author contributions.** HRB: conceptualization, formal analysis, methodology, investigation, and validation; AGH and EB: writing – review and editing; MNG: project administration and visualization; EF: laboratory analyses.

**Competing interests.** The contact author has declared that none of the authors has any competing interests.

**Disclaimer.** Publisher's note: Copernicus Publications remains neutral with regard to jurisdictional claims made in the text, published maps, institutional affiliations, or any other geographical representation in this paper. While Copernicus Publications makes every effort to include appropriate place names, the final responsibility lies with the authors.

**Acknowledgements.** This work was supported by the College of Agriculture and Natural Resources of Darab, Shiraz University, Darab, Iran.

**Review statement.** This paper was edited by Maria Jesus Gutierrez Gines and reviewed by Claudia Campillo-Cora and one anonymous referee.

## References

- Abdelhafez, A. A., Li, J., and Abbas, M. H.: Feasibility of biochar manufactured from organic wastes on the stabilization of heavy metals in a metal smelter contaminated soil, *Chemosphere*, 117, 66–71, 2014.
- Adrees, M., Ali, S., Rizwan, M., Zia-ur-Rehman, M., Ibrahim, M., Abbas, F., Farid, M., Qayyum, M. F., and Irshad, M. K.: Mechanisms of silicon-mediated alleviation of heavy metal toxicity in plants: a review, *Ecotox. Environ. Safe.*, 119, 186–197, 2015.
- Ahmad, M., Rajapaksha, A. U., Lim, J. E., Zhang, M., Bolan, N., Mohan, D., Vithanage, M., Lee, S. S., and Ok, Y. S.: Biochar as a sorbent for contaminant management in soil and water: a review, *Chemosphere*, 99, 19–33, 2014.
- Alam, M. S., Gorman-Lewis, D., Chen, N., Flynn, S. L., Ok, Y. S., Konhauser, K. O., and Alessi, D. S.: Thermodynamic analysis of nickel (II) and zinc (II) adsorption to biochar, *Environ. Sci. Technol.*, 52, 6246–6255, 2018.
- Anand, A., Gautam, S., and Ram, L. C.: Feedstock and pyrolysis conditions affect suitability of biochar for various sustainable energy and environmental applications, *J. Anal. Appl. Pyrol.*, 170, 105881, <https://doi.org/10.1016/j.jaap.2023.105881>, 2023.
- Ankita Rao, K., Nair, V., Divyashri, G., Krishna Murthy, T., Dey, P., Samrat, K., Chandraprabha, M., and Hari Krishna, R.: Role of Lignocellulosic Waste in Biochar Production for Adsorptive Removal of Pollutants from Wastewater, in: *Advanced and Innovative Approaches of Environmental Biotechnology in Industrial Wastewater Treatment*, Springer Nature Singapore, 221–238, [https://doi.org/10.1007/978-981-99-2598-8\\_2023](https://doi.org/10.1007/978-981-99-2598-8_2023).
- Antoniadis, V., Levizou, E., Shaheen, S. M., Ok, Y. S., Sebastian, A., Baum, C., Prasad, M. N., Wenzel, W. W., and Rinklebe, J.: Trace elements in the soil-plant interface: Phytoavailability, translocation, and phytoremediation—A review, *Earth-Sci. Rev.*, 171, 621–645, 2017.
- Bandara, T., Franks, A., Xu, J., Bolan, N., Wang, H., and Tang, C.: Chemical and biological immobilization mechanisms of potentially toxic elements in biochar-amended soils, *Crit. Rev. Env. Sci. Tec.*, 50, 903–978, 2020.
- Belton, D. J., Deschaume, O., and Perry, C. C.: An overview of the fundamentals of the chemistry of silica with relevance to biosilicification and technological advances, *FEBS J.*, 279, 1710–1720, 2012.
- Bharti, K. P., Pradhan, A. K., Singh, M., Beura, K., Behera, S. K., and Paul, S. C.: Effect of mycorrhizal co-Inoculation with selected rhizobacteria on soil zinc dynamics, *International Journal of Current Microbiology and Applied Sciences*, 7, 1961–1970, 2018.
- Bhat, J. A., Shivaraj, S., Singh, P., Navadagi, D. B., Tripathi, D. K., Dash, P. K., Solanke, A. U., Sonah, H., and Deshmukh, R.: Role of silicon in mitigation of heavy metal stresses in crop plants, *Plants*, 8, 71, <https://doi.org/10.3390/plants8030071>, 2019.
- Boostani, H., Hardie, A., Najafi-Ghiri, M., and Khalili, D.: Investigation of cadmium immobilization in a contaminated calcareous soil as influenced by biochars and natural zeolite application, *Int. J. Environ. Sci. Te.*, 15, 2433–2446, 2018.
- Boostani, H. R., Najafi-Ghiri, M., and Mirsoleimani, A.: The effect of biochars application on reducing the toxic effects of nickel and growth indices of spinach (*Spinacia oleracea* L.) in a calcareous soil, *Environ. Sci. Pollut. R.*, 26, 1751–1760, 2019a.
- Boostani, H. R., Najafi-Ghiri, M., Amin, H., and Mirsoleimani, A.: Zinc desorption kinetics from some calcareous soils of orange (*Citrus sinensis* L.) orchards, southern Iran, *Soil Sci. Plant Nutr.*, 65, 20–27, 2019b.
- Boostani, H. R., Hardie, A. G., Najafi-Ghiri, M., and Khalili, D.: The effect of soil moisture regime and biochar application on lead (Pb) stabilization in a contaminated soil, *Ecotox. Environ. Safe.*, 208, 111626, <https://doi.org/10.1016/j.ecoenv.2020.111626>, 2021.
- Boostani, H. R., Hardie, A. G., and Najafi-Ghiri, M.: Lead stabilization in a polluted calcareous soil using cost-effective biochar and zeolite amendments after spinach cultivation, *Pedosphere*, 33, 321–330, 2023a.
- Boostani, H. R., Hardie, A. G., and Najafi-Ghiri, M.: Chemical fractions, mobility and release kinetics of Cadmium in a light-textured calcareous soil as affected by crop residue biochars and Cd-contamination levels, *Chem. Ecol.*, 39, 525–538, <https://doi.org/10.1080/02757540.2023.2206807>, 2023b.
- Boostani, H. R., Hardie, A. G., Najafi-Ghiri, M., and Zare, M.: Chemical speciation and release kinetics of Ni in a Ni-contaminated calcareous soil as affected by organic waste biochars and soil moisture regime, *Environ. Geochem. Hlth.*, 45, 199–213, 2023c.
- Chatterjee, R., Sajjadi, B., Chen, W.-Y., Mattern, D. L., Hammer, N., Raman, V., and Dorris, A.: Effect of pyrolysis temperature on physicochemical properties and acoustic-based amination of biochar for efficient CO<sub>2</sub> adsorption, *Frontiers in Energy Research*, 8, 85, <https://doi.org/10.3389/fenrg.2020.00085>, 2020.
- Claoston, N., Samsuri, A., Ahmad Husni, M., and Mohd Amran, M.: Effects of pyrolysis temperature on the physicochemical properties of empty fruit bunch and rice husk biochars, *Waste Manage. Res.*, 32, 331–339, 2014.
- Dalal, R.: Comparative prediction of yield response and phosphorus uptake from soil using anion-and cation-anion-exchange resins, *Soil Sci.*, 139, 227–231, 1985.

- Dang, Y., Dalal, R., Edwards, D., and Tiller, K.: Kinetics of zinc desorption from Vertisols, *Soil Sci. Soc. Am. J.*, 58, 1392–1399, 1994.
- Deng, Y., Huang, S., Laird, D. A., Wang, X., and Meng, Z.: Adsorption behaviour and mechanisms of cadmium and nickel on rice straw biochars in single-and binary-metal systems, *Chemosphere*, 218, 308–318, 2019.
- Derakhshan Nejad, Z., Jung, M. C., and Kim, K.-H.: Remediation of soils contaminated with heavy metals with an emphasis on immobilization technology, *Environ. Geochem. Hlth.*, 40, 927–953, 2018.
- Dey, D., Sarangi, D., and Mondal, P.: Biochar: Porous Carbon Material, Its Role to Maintain Sustainable Environment, in: *Handbook of Porous Carbon Materials*, Springer Nature Singapore, 595–621, [https://doi.org/10.1007/978-981-19-7188-4\\_22](https://doi.org/10.1007/978-981-19-7188-4_22), 2023.
- El-Naggar, A., Rajapaksha, A. U., Shaheen, S. M., Rinklebe, J., and Ok, Y. S.: Potential of biochar to immobilize nickel in contaminated soils, in: *Nickel in Soils and Plants*, CRC Press, Taylor and Francis Group, 293–318, <https://doi.org/10.1201/9781315154664>, 2018.
- El-Naggar, A., Chang, S. X., Cai, Y., Lee, Y. H., Wang, J., Wang, S.-L., Ryu, C., Rinklebe, J., and Ok, Y. S.: Mechanistic insights into the (im) mobilization of arsenic, cadmium, lead, and zinc in a multi-contaminated soil treated with different biochars, *Environ. Int.*, 156, 106638, <https://doi.org/10.1016/j.envint.2021.106638>, 2021.
- Gao, W., He, W., Zhang, J., Chen, Y., Zhang, Z., Yang, Y., and He, Z.: Effects of biochar-based materials on nickel adsorption and bioavailability in soil, *Sci. Rep.*, 13, 8488, <https://doi.org/10.1038/s41598-023-35684-6>, 2023.
- Gee, G. W. and Bauder, J. W.: Particle-size analysis, in: *Methods of Soil Analysis: Part 1. Physical and Mineralogical Methods*, American Society of Agronomy, 5, 383–411, ISBN: 978-0891188117, 1986.
- Ghasemi-Fasaee, R., Maftoun, M., Ronaghi, A., Karimian, N., Yasrebi, J., Assad, M., and Ippolito, J.: Kinetics of copper desorption from highly calcareous soils, *Commun. Soil Sci. Plan.*, 37, 797–809, 2006.
- Ghiri, M. N., Abtahi, A., Owliaie, H., Hashemi, S. S., and Koohkan, H.: Factors affecting potassium pools distribution in calcareous soils of southern Iran, *Arid Land Res. Manag.*, 25, 313–327, 2011.
- Hossain, M. A., Piyatida, P., da Silva, J. A. T., and Fujita, M.: Molecular mechanism of heavy metal toxicity and tolerance in plants: central role of glutathione in detoxification of reactive oxygen species and methylglyoxal and in heavy metal chelation, *J. Bot.*, 2012, 1–37, <https://doi.org/10.1155/2012/872875>, 2012.
- Ippolito, J., Berry, C., Strawn, D., Novak, J., Levine, J., and Harley, A.: Biochars reduce mine land soil bioavailable metals, *J. Environ. Qual.*, 46, 411–419, 2017.
- Jalali, M., Beygi, M., Jalali, M., and Buss, W.: Background levels of DTPA-extractable trace elements in calcareous soils and prediction of trace element availability based on common soil properties, *J. Geochem. Explor.*, 241, 107073, <https://doi.org/10.1016/j.gexplo.2022.107073>, 2022.
- Kamali, S., Ronaghi, A., and Karimian, N.: Soil zinc transformations as affected by applied zinc and organic materials, *Commun. Soil Sci. Plan.*, 42, 1038–1049, 2011.
- Kameyama, K., Miyamoto, T., and Iwata, Y.: The preliminary study of water-retention related properties of biochar produced from various feedstock at different pyrolysis temperatures, *Materials*, 12, 1732, <https://doi.org/10.3390/ma12111732>, 2019.
- Kandpal, G., Srivastava, P., and Ram, B.: Kinetics of desorption of heavy metals from polluted soils: Influence of soil type and metal source, *Water Air Soil Poll.*, 161, 353–363, 2005.
- Keiluweit, M., Nico, P. S., Johnson, M. G., and Kleber, M.: Dynamic molecular structure of plant biomass-derived black carbon (biochar), *Environ. Sci. Technol.*, 44, 1247–1253, 2010.
- Khalique, A., Ali, S., Hameed, A., Farooq, M. A., Farid, M., Shakoor, M. B., Mahmood, K., Ishaque, W., and Rizwan, M.: Silicon alleviates nickel toxicity in cotton seedlings through enhancing growth, photosynthesis, and suppressing Ni uptake and oxidative stress, *Arch. Agron. Soil Sci.*, 62, 633–647, 2016.
- Li, X.: Technical solutions for the safe utilization of heavy metal-contaminated farmland in China: a critical review, *Land Degrad. Dev.*, 30, 1773–1784, 2019.
- Liang, Y., Wong, J., and Wei, L.: Silicon-mediated enhancement of cadmium tolerance in maize (*Zea mays* L.) grown in cadmium contaminated soil, *Chemosphere*, 58, 475–483, 2005.
- Lindsay, W. L. and Norvell, W.: Development of a DTPA soil test for zinc, iron, manganese, and copper, *Soil Sci. Soc. Am. J.*, 42, 421–428, 1978.
- Liu, L., Guo, X., Wang, S., Li, L., Zeng, Y., and Liu, G.: Effects of wood vinegar on properties and mechanism of heavy metal competitive adsorption on secondary fermentation based composts, *Ecotox. Environ. Safe.*, 150, 270–279, 2018.
- Loeppert, R. H. and Suarez, D. L.: Carbonate and gypsum, in: *Methods of Soil Analysis: Part 3 Chemical Methods*, 5, 437–474, 1996.
- Lu, K., Yang, X., Gielen, G., Bolan, N., Ok, Y. S., Niazi, N. K., Xu, S., Yuan, G., Chen, X., and Zhang, X.: Effect of bamboo and rice straw biochars on the mobility and redistribution of heavy metals (Cd, Cu, Pb and Zn) in contaminated soil, *J. Environ. Manage.*, 186, 285–292, 2017.
- Ma, C., Ci, K., Zhu, J., Sun, Z., Liu, Z., Li, X., Zhu, Y., Tang, C., Wang, P., and Liu, Z.: Impacts of exogenous mineral silicon on cadmium migration and transformation in the soil-rice system and on soil health, *Sci. Total Environ.*, 759, 143501, <https://doi.org/10.1016/j.scitotenv.2020.143501>, 2021.
- Mailakeba, C. D. and BK, R. R.: Biochar application alters soil Ni fractions and phytotoxicity of Ni to pakchoi (*Brassica rapa* L. ssp. *chinensis* L.) plants, *Environmental Technology & Innovation*, 23, 101751, <https://doi.org/10.1016/j.eti.2021.101751>, 2021.
- Maruyama, M., Sawada, K. P., Tanaka, Y., Okada, A., Momma, K., Nakamura, M., Mori, R., Furukawa, Y., Sugiura, Y., and Tajiri, R.: Quantitative analysis of calcium oxalate monohydrate and dihydrate for elucidating the formation mechanism of calcium oxalate kidney stones, *PLOS ONE*, 18, e0282743, <https://doi.org/10.1371/journal.pone.0282743>, 2023.
- Maryam, H., Abbasi, G. H., Waseem, M., Ahmed, T., and Rizwan, M.: Preparation and characterization of green silicon nanoparticles and their effects on growth and lead (Pb) accumulation in maize (*Zea mays* L.), *Environ. Pollut.*, 346, 123691, <https://doi.org/10.1016/j.envpol.2024.123691>, 2024.
- Myszka, B., Schüßler, M., Hurler, K., Demmert, B., Detsch, R., Boccaccini, A. R., and Wolf, S. E.: Phase-specific bioactivity and

- altered Ostwald ripening pathways of calcium carbonate polymorphs in simulated body fluid, *RSC Adv.*, 9, 18232–18244, 2019.
- Nasrabadi, M., Omid, M. H., and Mazdeh, A. M.: Experimental Study of Flow Turbulence Effect on Cadmium Desorption Kinetics from Riverbed Sands, *Environmental Processes*, 9, 10, <https://doi.org/10.1007/s40710-022-00558-y>, 2022.
- Nelson, D. W. and Sommers, L. E.: Total carbon, organic carbon, and organic matter, in: *Methods of Soil Analysis: Part 3 Chemical Methods*, American Society of Agronomy, 5, 961–1010, ISBN: 978-0891188254, 1996.
- Poznanović Spahić, M. M., Sakan, S. M., Glavaš-Trbić, B. M., Tančić, P. I., Škrivanj, S. B., Kovačević, J. R., and Manojlović, D. D.: Natural and anthropogenic sources of chromium, nickel and cobalt in soils impacted by agricultural and industrial activity (Vojvodina, Serbia), *J. Environ. Sci. Heal. A*, 54, 219–230, 2019.
- Rassaei, F., Hoodaji, M., and Abtahi, S. A.: Fractionation and mobility of cadmium and zinc in calcareous soils of Fars Province, Iran, *Arab. J. Geosci.*, 13, 1–7, 2020.
- Rhoades, J.: Salinity: Electrical conductivity and total dissolved solids, *Methods of Soil Analysis: Part 3 Chemical Methods*, 5, 417–435, 1996.
- Rizwan, M., Ali, S., Qayyum, M. F., Ibrahim, M., Zia-ur-Rehman, M., Abbas, T., and Ok, Y. S.: Mechanisms of biochar-mediated alleviation of toxicity of trace elements in plants: a critical review, *Environ. Sci. Pollut. R.*, 23, 2230–2248, 2016.
- Sachdeva, S., Kumar, R., Sahoo, P. K., and Nadda, A. K.: Recent advances in biochar amendments for immobilization of heavy metals in an agricultural ecosystem: A systematic review, *Environ. Pollut.*, 319, 120937, 2023.
- Saffari, M., Karimian, N., Ronaghi, A., Yasrebi, J., and Ghasemi-Fasaei, R.: Stabilization of nickel in a contaminated calcareous soil amended with low-cost amendments, *J. Soil Sci. Plant Nut.*, 15, 896–913, 2015.
- Sajadi Tabar, S. and Jalali, M.: Kinetics of Cd release from some contaminated calcareous soils, *Natural Resources Research*, 22, 37–44, 2013.
- Shahbazi, K., Marzi, M., and Rezaei, H.: Heavy metal concentration in the agricultural soils under the different climatic regions: a case study of Iran, *Environ. Earth Sci.*, 79, 324, <https://doi.org/10.1007/s12665-020-09072-6>, 2020.
- Shahbazi, K., Fathi-Gerdeldani, A., and Marzi, M.: Investigation of the status of heavy metals in soils of Iran: A comprehensive and critical review of reported studies, *Iranian Journal of Soil and Water Research*, 53, 1163–1212, <https://doi.org/10.22059/ijswr.2022.341586.669245>, 2022.
- Shahzad, B., Tanveer, M., Rehman, A., Cheema, S. A., Fahad, S., Rehman, S., and Sharma, A.: Nickel; whether toxic or essential for plants and environment – A review, *Plant Physiol. Bioch.*, 132, 641–651, 2018.
- Shen, B., Wang, X., Zhang, Y., Zhang, M., Wang, K., Xie, P., and Ji, H.: The optimum pH and Eh for simultaneously minimizing bioavailable cadmium and arsenic contents in soils under the organic fertilizer application, *Sci. Total Environ.*, 711, 135229, <https://doi.org/10.1016/j.scitotenv.2019.135229>, 2020.
- Singh, J., Karwasra, S., and Singh, M.: Distribution and forms of copper, iron, manganese, and zinc in calcareous soils of India, *Soil Sci.*, 146, 359–366, 1988.
- Sparks, D. L., Singh, B., and Siebecker, M. G.: *Environmental soil chemistry*, Elsevier, Academic Press, eBook ISBN: 9780443140358, 2022.
- Sparrow, L. and Uren, N.: Manganese oxidation and reduction in soils: effects of temperature, water potential, pH and their interactions, *Soil Res.*, 52, 483–494, 2014.
- Sumner, M. E. and Miller, W. P.: Cation exchange capacity and exchange coefficients, in: *Methods of Soil Analysis: Part 3 Chemical Methods*, 5, 1201–1229, 1996.
- Sun, L., Zhang, G., Li, X., Zhang, X., Hang, W., Tang, M., and Gao, Y.: Effects of biochar on the transformation of cadmium fractions in alkaline soil, *Heliyon*, 9, e12949, <https://doi.org/10.1016/j.heliyon.2023.e12949>, 2023.
- Sun, Y., Gao, B., Yao, Y., Fang, J., Zhang, M., Zhou, Y., Chen, H., and Yang, L.: Effects of feedstock type, production method, and pyrolysis temperature on biochar and hydrochar properties, *Chem. Eng. J.*, 240, 574–578, 2014.
- Tomczyk, A., Sokołowska, Z., and Boguta, P.: Biochar physicochemical properties: pyrolysis temperature and feedstock kind effects, *Rev. Environ. Sci. Bio.*, 19, 191–215, 2020.
- Uchimiya, M., Lima, I. M., Thomas Klasson, K., Chang, S., Wartelle, L. H., and Rodgers, J. E.: Immobilization of heavy metal ions (CuII, CdII, NiII, and PbII) by broiler litter-derived biochars in water and soil, *J. Agr. Food Chem.*, 58, 5538–5544, 2010.
- Vickers, N. J.: Animal Communication: When I'm Calling You, Will You Answer Too?, *Curr. Biol.*, 27, R713–R715, 2017.
- Xiao, Z., Peng, M., Mei, Y., Tan, L., and Liang, Y.: Effect of organosilicone and mineral silicon fertilizers on chemical forms of cadmium and lead in soil and their accumulation in rice, *Environ. Pollut.*, 283, 117107, 2021.
- Yan, G.-C., Nikolic, M., Ye, M.-J., Xiao, Z.-X., and Liang, Y.-C.: Silicon acquisition and accumulation in plant and its significance for agriculture, *J. Integr. Agr.*, 17, 2138–2150, 2018.
- Yuan, J.-H., Xu, R.-K., and Zhang, H.: The forms of alkalis in the biochar produced from crop residues at different temperatures, *Bioresource Technol.*, 102, 3488–3497, 2011.
- Zemnukhova, L. A., Panasenko, A. E., Artem'yanov, A. P., and Tsoy, E. A.: Dependence of porosity of amorphous silicon dioxide prepared from rice straw on plant variety, *BioResources*, 10, 3713–3723, 2015.
- Zeng, X., Xiao, Z., Zhang, G., Wang, A., Li, Z., Liu, Y., Wang, H., Zeng, Q., Liang, Y., and Zou, D.: Speciation and bioavailability of heavy metals in pyrolytic biochar of swine and goat manures, *J. Anal. Appl. Pyrol.*, 132, 82–93, 2018.
- Zhao, S.-X., Ta, N., and Wang, X.-D.: Effect of temperature on the structural and physicochemical properties of biochar with apple tree branches as feedstock material, *Energies*, 10, 1–15, 2017.
- Zhu, Q., Wu, J., Wang, L., Yang, G., and Zhang, X.: Effect of biochar on heavy metal speciation of paddy soil, *Water Air Soil Pollut.*, 226, 1–10, 2015.